Phase Structural Transitions of Polyelectrolyte−Surfactant Complexes between Poly(vinylamine hydrochloride) and Oppositely Charged Sodium Alkyl Sulfate

Shuiqin Zhou, Haibo Hu, Christian Burger, and Benjamin Chu*

Department of Chemistry, State University of New York at Stony Brook, Stony Brook, New York 11794-3400

Received July 21, 2000; Revised Manuscript Received December 7, 2000

ABSTRACT: Synchrotron small-angle X-ray scattering was used to investigate the nanostructures of polyelectrolyte−surfactant complexes between linear poly(vinylamine hydrochloride) chains and oppositely charged surfactants of sodium alkyl sulfate (SC_nS) at room temperature (~23 °C). Both the pH variance of complexation and the surfactant tail length change could induce phase structural transitions. A novel phase structure of a 2D distorted hexagonal packing of deformed cylinders or ribbons with $a = b$ and an enclosed angle θ larger than 120° was, for the first time, observed in polyelectrolyte−surfactant complexes at $n = 11-12$ and certain pH values. In sequence with increasing pH values of complexation between the PVACl and $SC_{11}S$ solutions from pH = 5.9 to pH = 12.0, the structures of 2D distorted hexagonal, bilayer lamellar, and 2D hexagonal close packing of cylinders were determined. When the pH values for complexation were fixed at 5.9 and 8.9, the decrease in carbon atom numbers of surfactant alkyl chains from $n = 12$ to $n = 9$ induced the same structural transition. This structural transition was caused by the increase in the ratio of the area of polar groups to the volume of alkyl chains of surfactants arranged inside the complexes, thus increasing the mean curvature at the polar/apolar interfaces of surfactant ions. The increase in surfactant tail length could also induce a lamellar structural transition. When the lamellar structure in complexes was formed by SC_nS with $n = 10$ and 11, the alkyl chains of surfactant were fully extended and perpendicular to the lamellar surface, while when the lamellar structure in complexes was formed by SC_nS with long tails of $n = 14$ and 16, the alkyl chains of surfactant were partially overlapped or tilted to the lamellar surface in the bilayer arrangement due to the stronger hydrophobic interactions.

Introduction

Self-assembly is defined as spontaneous intermolecular association via noncovalent bonds, e.g., electrostatic interactions, hydrogen bonds, or hydrophobic interactions, resulting in thermodynamically stable, well-defined supramolecular structures.[1] Control over the organization of supramolecular structures by tuning the assembly processes opens fascinating possibilities in the manipulation of materials properties on a molecular scale. This may be particularly important for technological applications, such as electronic devices, microsensors, separation membranes, catalysts, and biomaterials.[2,3] The complexes between polyelectrolytes and oppositely charged surfactants are the best-known self-assembly polymeric systems.[4,5] Such complexes can exhibit liquid crystalline mesophase characteristics of the bound surfactants, while the threading of polyelectrolyte chains through the mesophases of surfactant/water binary systems may create different geometrical constraints from a small molecule, thus having the possibility to produce new ordered structures.[2,3]

When polyelectrolyte and oppositely charged surfactant aqueous solutions are mixed, the complexes can be formed spontaneously. Surfactant molecules aggregate to form micelles at a concentration considerably lower than their critical micelle concentration (cmc) during the complexation and are highly cooperative with polymer chains. A highly charged polyelectrolyte can release some of its condensed counterions when it binds to the micelle.[6] The electrostatic driving force for complexation can be reinforced by hydrophobic self-association of the surfactant tails in water. Various techniques have been used to study the formations, structures, and properties of polyelectrolyte−surfactant complexes.[2−5,7−9]

Substantial efforts have been made to clarify the structures of polyelectrolyte−surfactant complexes.[2,3,10−14] Okuzaki and Osada[10] proposed a simple cubic structure for the complexes formed by poly(2-acrylamido-2-methylpropanesulfonic acid) and alkylpyridinium chloride. Khokhlov et al.[11] have studied the ionic strength effect on the highly ordered lamellar structure in gel−surfactant complexes between poly(diallyldimethylammonium chloride) and sodium dodecylbenzenesulfonate. Antonietti et al.[12−14] have investigated the solid-state structures of various polyelectrolyte−surfactant complexes. Lamellar, modulated-lamellar, face-centered-cubic packing of undulated cylinders, hexagonal packing of cylinders, and bicontinuous sponge phase structures have been observed and analyzed.

In our laboratory in the past 5 years, synchrotron small-angle X-ray scattering (SAXS) has been used to investigate the nanostructures of various polyelectrolyte−surfactant complexes. In complexes between cationic gels of poly(diallyldimethylammonium chloride) (PDADMACl) and anionic surfactants of sodium alkyl sulfate (SC_nS), the decrease in surfactant tail length could induce a structural transition from a two-dimensional (2D) hexagonal structure to $Pm3n$ cubic structure,[15,16] while in complexes between anionic hydrogels of poly(*N*-isopropylacrylamide-*co*-sodium methacrylate) [P(NIPAM-*co*-MAA)] and alkyltrimethylammonium bromide (C_nTAB), the decrease in charge density of polyelectrolyte chains could induce a structural transition from $Pm3n$ cubic to face-centered cubic and then to a

10.1021/ma001277m CCC: $20.00
Published on Web 02/10/2001

3D hexagonal close packing of spheres.[17,18] The structural formation and transition of the complexes were also examined in terms of the hydrophobicity and backbone flexibility of polyelectrolyte chains and the surfactant tail length.[19] Very recently, we have started a new system of polyelectrolyte−surfactant complexes between poly(vinylamine hydrochloride) (PVACl) and sodium alkyl sulfate (SC_nS). A pH-induced structural transition in the PVACl−$SC_{10}S$ complex from *Ia*3*d* cubic to bilayer lamellar and then to 2D hexagonal close packing of cylinders was, for the first time, reported.[20] These phase structures are also believed to occur as intermediate structures during biological processes, e.g., cell fusion, because both DNA and proteins are polyelectrolytes.[21]

In this paper, we systematically present novel phase structures and structural transitions in PVACl−SC_nS complexes formed at different pH values (pH = 5.9−12.0) and different surfactant tail lengths (n = 9−16). The novel phase structure of a 2D distorted hexagonal packing of deformed cylinders or ribbons with $a = b$ and an enclosed angle θ larger than 120° was analyzed in detail. The structural transition from 2D distorted hexagonal to bilayer lamellar and then to 2D hexagonal phase induced by both increase in pH values and decrease in surfactant tail length for complexation was discussed. The two different lamellar structures resulting from the difference in surfactant tail length for complexation were also compared.

Experimental Section

Materials. Poly(vinylamine hydrochloride) (PVACl) was purchased from Polyscience, Inc., with M_w = 25 000 g/mol. The surfactants of sodium alkyl sulfate (SC_nS) with n = 9−16 (Lancaster, 99%) were used without further purification. Deionized water was distilled before use. Hydrochloric acid (36.9%) and sodium hydroxide (6.25 N) from Fisher Scientific were diluted and used to adjust pH values of PVACl and SC_nS solutions.

Preparation of PVACl−SC_nS Complexes. Complexes were prepared by adding the PVACl aqueous solution dropwise to the SC_nS aqueous solution at desired pH values and room temperature under stirring conditions. The PVACl or SC_nS solutions were prepared in very dilute HCl or NaOH aqueous solution in order to achieve the correct pH values. The concentration of PVACl was fixed at 1 mg/mL, while the concentrations of SC_nS solutions were kept at $^1/_3$ critical micelle concentration (cmc). The volumes of the surfactant solutions were controlled at such a level that the ratio r, defined by ⟨number of surfactant molecules in solution⟩/⟨number of charged sites in the polymer chains in solution⟩, was in the range of r = 1.5. It means that the number of surfactant molecules was always in excess of the number of charged groups in the polymer chain for complexation. After complexation between PVACl and SC_nS solutions, the mixed solution became slightly cloudy. The complex particles gradually precipitated from the solutions after being settled at room temperature for 1 week. After being equilibrated with the external surfactant solution for another 2 weeks, the complexes were collected for SAXS measurements.

X-ray Scattering Measurements. Small-angle X-ray scattering (SAXS) measurements were carried out at the Advanced Polymers Beam Line X27C at the National Synchrotron Light Source, Brookhaven National Laboratory, using a laser-aided prealigned pinhole collimator.[22] The incident beam wavelength (λ) was tuned at 0.1307 nm. A 2D imaging plate was used in conjunction with an image scanner as the detection system. The sample-to-detector distance was 911 mm, corresponding to a q range of $0.6 \le q \le 5.2$ nm^{-1} with $q = (4\pi/\lambda)\sin(\theta/2)$ and θ being the scattering angle between the incident and the scattered X-rays. The experimental data were corrected for background scattering and sample transmission. Smearing due to collimation effects was negligible for this setup.

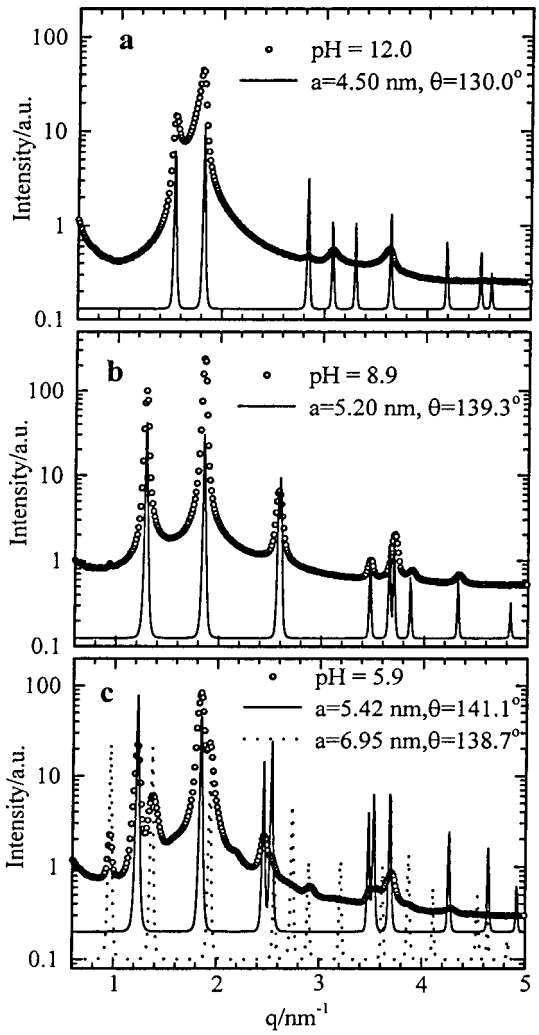

Figure 1. Typical SAXS profiles of the PVACl−$SC_{12}S$ complexes formed at three different pH values of (a) pH = 12.0, (b) pH = 8.9, and (c) pH = 5.9. The solid and dotted lines represent the simulation curves from the 2D distorted hexagonal structural model, as shown in Figure 2, with different lattice parameters.

Results and Discussion

The PVACl−SC_nS complex particles precipitated in the bottom of the container were viscous, semitransparent, and solidlike. The complexes were always kept in equilibrium with the external surfactant solutions even during the SAXS measurements. The concentrations of SC_nS were fixed at $^1/_3$ cmc. Thus, there were no micellar aggregates being formed in the surfactant solution before being complexed with PVACl chains. Because the molar ratio of SC_nS to the polymer charge units was fixed at 1.5 for complexation, it was possible that some excess surfactant molecules could be adsorbed on the surface of neutralized complex precipitates. For long-tailed surfactants, the concentration of external surfactant solution was very low (~10^{-4} M); thus, the adsorption of surfactant molecules to the surface of complex particles could be reduced.

I. PVACl−$SC_{12}S$ Complexes: Novel 2D Distorted Hexagonal Phase Structure. Figure 1 shows three typical SAXS profiles of the PVACl−$SC_{12}S$ complexes formed at pH = 12.0 (a), 8.9 (b), and 5.9 (c). A fairly

large number of well-resolved peaks can be observed that do not follow any of the well-known simple peak position ratios of the classical morphologies like 1:2:3:4 for lamellar or $1:3^{1/2}:2:7^{1/2}$ for 2D hexagonal symmetry. Furthermore, the observed peak positions also do not fit into a cubic indexing scheme where $q_{hkl} = 2\pi a^{-1}(h^2 + k^2 + l^2)^{1/2}$ with the lattice constant a being the single free parameter of this symmetry. Thus, these classical morphologies can be ruled out, and the present structure will require at least two free parameters among its lattice constants to account for the observed variability of the peak positions.

Possible candidates for structures with two free lattice parameters in a 2D system are any nonhexagonal and nonquadratic packings where either the two edges of the unit cell are different or the enclosed angle θ is different from 120° and different from 90°. The combination of the edge and the angle condition leads to a three-parameter system. Possible two-parameter systems in 3D are a hexagonal unit cell with a finite height or a tetragonal system. Going beyond two parameters, the number of possible symmetries increases quickly.

To find the correct morphology, we start with the 2D systems with two free parameters and compare the experimentally observed scattering curves with calculated data, varying the two free parameters by trial and error. The calculated scattering curves shown in Figure 1 do not attempt to completely fit all features of the experimental curves but essentially consist of the crystallographic lattice factor so that the peak positions can be compared. We write

$$I(q) = \langle \sum_{h,k} I_{hk}(|q - ha^* - kb^*|) \rangle_\omega \equiv \sum_{h,k>0} \frac{m_{hk}}{4\pi q_{hk}^2} I_{hk}(q - q_{hk})$$

where h and k are Miller indices in 2D, a^* and b^* are base vectors in 2D reciprocal space, I_{hk} is a normalized peak shape profile, $\langle\ \rangle_\omega$ stands for a spherical average, and m_{hk} is the multiplicity, i.e., the number of reciprocal lattice points with the same absolute q lumped together after the spherical averaging. The peak shape profile I_{hk} defines a certain peak width depending on crystallite sizes, lattice distortions, and collimation aspects that need not be a constant in q. However, for the present calculations, a small constant peak width has been used in a Lorentzian peak profile. In the present framework, we do not consider the exact crystallographic structure factor. This means, while calculated and experimental peak positions should coincide with a perfect match, the calculated peak intensities should be considered as a rough hint based on the multiplicity only. It should be noted that the experimental peak positions can be measured with very high accuracy and that the calculated peak positions are very sensitive to small changes in the parameters so that the lattice constants obtained from the procedure are significant to a fraction of an angstrom for lengths and to a fraction of a degree for angles, respectively.

On the basis of this approach, we find that the present structures can be very well described with a nonhexagonal 2D unit cell with two equal edges $a = b$ and an enclosed angle θ different from 120° and, more specifically, larger than 120°. The cross section of this structure is sketched in Figure 2.

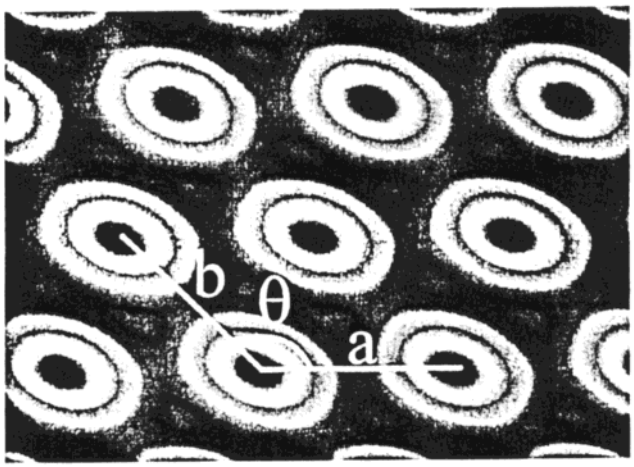

Figure 2. A possible structural model of 2D distorted hexagonal packing of deformed cylinders, e.g., ellipsoidals.

Since our calculation did not consider the crystallographic structure factor, it does not provide first-hand information about the contents of this 2D unit cell. On the basis of a comparison with the usual hexagonally packed cylinder systems, we suggest that these systems also consist of a packing of cylindrical structural units where, however, the cross section of the cylinders need no longer be circular but could be elliptical in order to account for the overall distortion of the system.

Comparing experimental and calculated scattering curves in Figure 1a,b, we see a very good agreement of the peak positions. Since we experimentally observe about five to seven well-resolved peaks and our model consists only of two free parameters, the proposed structure assignment has a very high level of confidence.

A qualitative inspection of the experimental scattering curves shows the characteristic feature that the second peak is significantly more intense than the first peak. This is quite unusual and not found in most of the classical morphologies. It can be easily understood by generating the present structure through a deformation from a hexagonal system. In a 2D hexagonal system, the first and most intense peak has a multiplicity of 6, consisting of the Miller indices (01), (10), (0$\bar{1}$), ($\bar{1}$0), (1$\bar{1}$), and ($\bar{1}$1). If the hexagonal symmetry is distorted, this single first peak splits up. If the distortion is such that we have two equal edges and an enclosed angle larger than 120°, the hexagonal peak with a multiplicity of 6 splits up into a peak at lower angles with the multiplicity of 2, consisting of the indices (1$\bar{1}$) and ($\bar{1}$1), and a peak at higher angles with a multiplicity of 4, consisting of the indices (01), (10), (0$\bar{1}$), and ($\bar{1}$0). Thus, neglecting the structure factor and the spherical average, we expect the second peak to have roughly twice the intensity of the first peak for this symmetry. If the enclosed angle is less than 120°, the situation is reversed, and the first peak has the multiplicity of 4 and, thus, the higher intensity. If, in addition to the angle $\theta \neq 120°$, the two edges are different, $a \neq b$, then the first hexagonal peak splits into three peaks, each having a multiplicity of two. In all these cases, the angle $\theta \neq 120°$ is a continuously variable parameter so that there is no fixed peak position ratio between the split-up subpeaks. All higher-order peaks undergo a similar split, so that the resulting scattering curves have their observed complicated appearance.

After this explanation let us consider the experimental SAXS curve in Figure 1c. We observe more than 10

peaks with no apparent pattern between their positions and also their intensities, as now the fourth peak is the most intense. However, with the help of some imagination, we are able to observe the characteristic pattern of two peaks with the second peak being roughly twice as intense. In this case, it just appears as an overlay of two different curves. Calculating the corresponding higher-order peaks shows a good agreement so that, having fit more than 10 peaks with four free parameters, this structure proposal can also be considered highly confident. Apparently, at a pH of 5.9, we have a macroscopic phase separation into two independent scattering domains, each forming a similar 2D distorted hexagonal structure, but with different lattice constants. It is not clear what caused this phase separation and whether this is a stable state.

Clearly, all three PVACl−$SC_{12}S$ complexes formed at pH = 5.9, 8.9, and 12.0 showed the same structure of 2D distorted hexagonal, but with different dimensions of deformed cylinders and packing angles. By increasing the pH values for complexation between PVACl and $SC_{12}S$ solutions, both a and θ decreased. The decrease in dimensions of deformed cylinders and packing angles could be attributed to the reduced charge density of PVA chains when pH was gradually increased from 5.9 to 12.0. At pH = 5.9, most of the amine groups can be protonated, so the charge density of the PVA chains is very high. Furthermore, the $-NH_3^+$ groups are very close to the PVA backbone chains; thus, the $C_{12}S$ ions bound by PVA chains would pack very densely, and the formed cylindrical micelles could be deformed with an elliptical shape in cross section because of the space hindrance. With increasing pH values, the charge density of PVA chains decreased so that the number density of $C_{12}S$ ions bound by PVA chains in unit volume decreased. The self-assembly of these bound surfactant ions would produce a relatively smaller radial dimension and less-deformed cylindrical micelles. The packing of these smaller and less-deformed cylinders or ribbons led to a 2D distorted hexagonal structure with less deviation of the packing angle θ from 120° as shown in a standard 2D hexagonal structure packed by cylinders.

The 2D distorted hexagonal structures observed in our PVACl−$SC_{12}S$ complexes ($a = b$) showed higher symmetry than the usual 2D monoclinic phase M_α observed in some surfactant/water binary systems,[23,24] in which the two edges were nonequal ($a \neq b$). Although the 2D monoclinic phase M_α has been observed in the $SC_{12}S$/water binary system at high $SC_{12}S$ concentrations (58−62 wt %) and high temperatures (>40 °C), the 2D distorted hexagonal packing structure with $a = b$ and $\theta > 130°$ was never presented in the whole phase diagram of $SC_{12}S$/water binary system. Furthermore, the structures of 2D distorted hexagonal packing with $a = b$ and $\theta > 130°$ in the PVACl−$SC_{12}S$ complexes were produced at room temperature and very dilute $SC_{12}S$ concentrations ($\sim 1/3$ cmc). Obviously, the threading and constraints of densely charged PVA chains in the $SC_{12}S$ aqueous solution could produce new phase structures even under easily accessible conditions.

II. PVACl−$SC_{11}S$ Complexes: pH-Induced Structural Transition. Figure 3 shows the SAXS profiles of PVACl−$SC_{11}S$ complexes formed at pH = 5.9 (a), 8.9 (b), and 12.0 (c). When the complex was formed at pH = 5.9, seven scattering peaks were observed but did not show a simple spacing ratio. However, all the peaks can be fitted by a 2D distorted hexagonal packing of

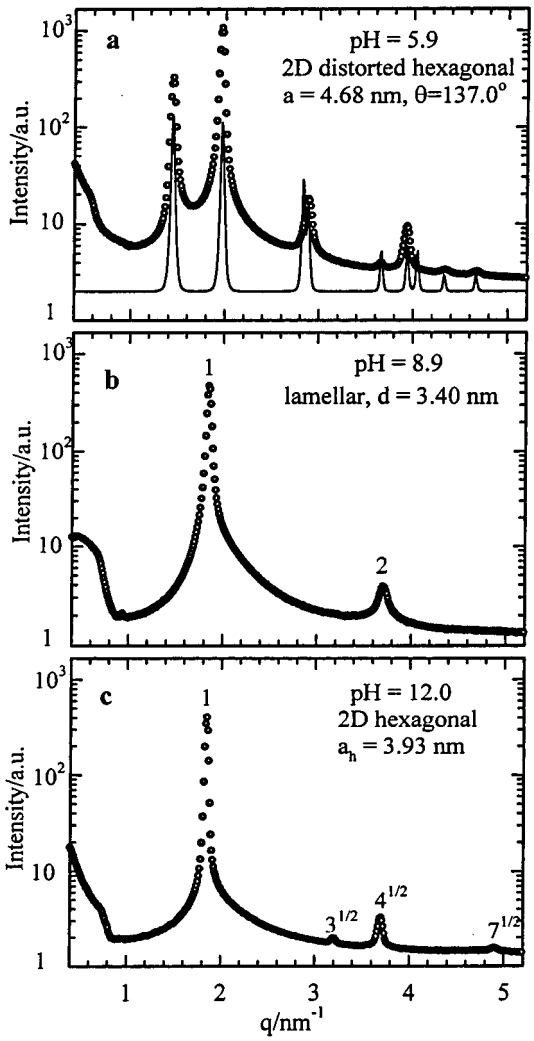

Figure 3. Typical SAXS profiles of the PVACl−$SC_{11}S$ complexes formed at three different pH values of (a) pH = 5.9, (b) pH = 8.9, and (c) pH = 12.0. The increase in pH values induced a structural transition from 2D distorted hexagonal to lamellar and then to 2D hexagonal structure.

deformed cylinders or ribbons. The solid curve in Figure 3a represents the calculated curve based on the structural model, as shown in Figure 2, with lattice parameters of $a = b = 4.68$ nm and $\theta = 137.0°$. When the PVACl−$SC_{11}S$ complex formed at pH = 8.9, the SAXS curve became much simpler. Two scattering peaks at $q = 1.85$ and 3.70 nm^{-1} were observed, which could be indexed as the 001 and 002 planes of a layered structure. An interlayer spacing of 3.40 nm indicated a bilayer arrangement of the $C_{11}S$ ions intercalated by PVA chains. By further increasing the pH value of complexation between PVACl and $SC_{11}S$ solutions to 12.0, very sharp scattering peaks with a spacing ratio of $1:3^{1/2}:2:7^{1/2}$ were observed, indicating that a structure of 2D hexagonal close packing of cylinders was formed. Obviously, the gradual increase in pH values from 5.9 to 12.0 for complexation between PVACl and $SC_{11}S$ solutions has induced a phase transition of the complexes from a 2D distorted hexagonal structure to a multibilayer lamellar structure and finally to a 2D hexagonal close packing of cylinders.

How could the increase in pH values of complexation lead to the structural transition? The increase in pH value of PVACl solution would decrease the charge density on PVA chains. When the charge sites of PVA

Table 1. Structures of PVACl−SC_nS Complexes Formed at Different pH Values and Alkyl Chain Length of Surfactant

	PVACl−$SC_{12}S$	PVACl−$SC_{11}S$	PVACl−$SC_{10}S$	PVACl−SC_9S
pH = 12.0	2D distorted hexagonal	hexagonal	hexagonal	hexagonal
pH = 8.9	2D distorted hexagonal	lamellar	lamellar	hexagonal
pH = 5.9	2D distorted hexagonal	2D distorted hexagonal	lamellar	hexagonal

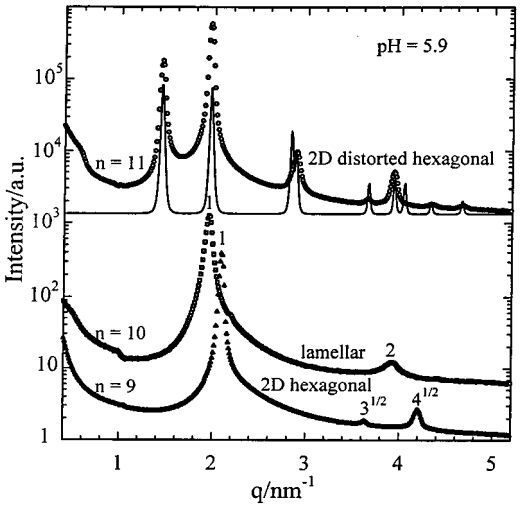

Figure 4. Typical SAXS profiles of the PVACl−SC_nS complexes formed at pH = 5.9, but three different *n* values of 9, 10, and 11. The decrease in *n* values of surfactants induced a structural transition from 2D distorted hexagonal to lamellar and then to 2D hexagonal structure.

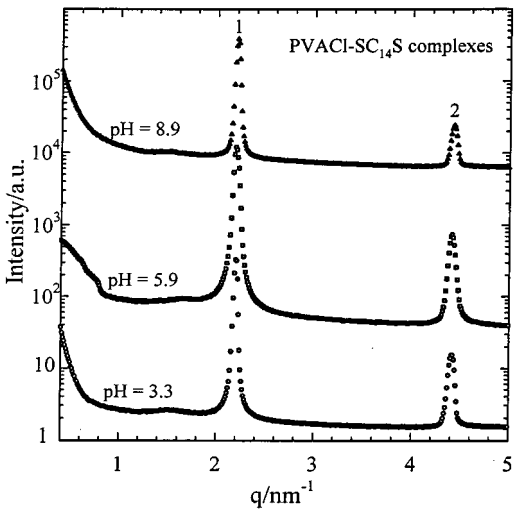

Figure 5. Typical SAXS profiles of the PVACl−$SC_{14}S$ complexes formed at three different pH values of 3.3, 5.9, and 8.9.

chains were neutralized by $C_{11}S$ ions and became hydrophobic, the originally neutral sites were still hydrophilic and favored the aqueous phase. Therefore, when the charge density of PVA chains was reduced, the amount of water molecules available for the headgroups of surfactants was increased, thus increasing the ratio of the area of headgroup to the volume of tail of the surfactant. In other words, the mean interfacial curvature between the hydrophilic moieties and the hydrophobic tails of surfactant in the complexes increased with an increase in pH values of complexation. The pH-induced increase in interfacial curvature of surfactant could explain the structural transition from the 2D distorted hexagonal to lamellar and then to 2D hexagonal structure. The lamellar phase has a zero mean curvature because the surface is essentially flat; thus, the 2D distorted hexagonal would have a negative curvature, and the 2D hexagonal should have a positive curvature.[25] It means that the 2D distorted hexagonal structure had an inverse phase with surfactant layer curling toward the hydrophobic tail region, while the 2D hexagonal structure had a normal phase with the curvature toward the hydrophilic phase of PVA chains, sulfate groups of $C_{11}S$ ions, and water and the hydrophobic undecyl chains filled inside the cylinders.

III. PVACl−SC_nS Complexes Formed at Fixed pH Values: Surfactant Tail Length-Induced Structural Transition. Figure 4 shows the SAXS profiles of PVACl−SC_nS complexes formed at pH = 5.9 but different *n* values (*n* = 9−11). As shown above, the PVACl−$SC_{11}S$ complex formed at pH = 5.9 produced a 2D distorted hexagonal structure. When the *n* decreased from 11 to 10, the SAXS curve from the PVACl−$SC_{10}S$ complex showed only two scattering peaks with a spacing ratio of 1:2, indicating a lamellar structure had been formed. The interlayer spacing was calculated to be 3.22 nm. Further decreasing *n* from 10 to 9, the SAXS curve from the PVACl−SC_9S complex changed again. Three scattering peaks with a spacing ratio of $1:3^{1/2}:2$ were observed, indicating that a 2D hexagonal structure was formed. Clearly, the decrease in surfactant tail length (carbon atom number *n*) could also induce a structural transition in complexes from 2D distorted hexagonal to lamellar and then to a 2D hexagonal structure. This surfactant tail shortening induced structural transition at a fixed pH value is exactly the same as the pH increase induced structural transition at a fixed surfactant tail length. What is their common feature? As discussed previously, an increase in pH values of complexation increased the mean interfacial curvature of the surfactant in complexes. Similarly, the decrease in surfactant tail length would also increase the ratio of the area of headgroup to the volume of tail of surfactant, thus increasing the mean curvature of surfactant in the complexes[26] and thereby leading to the same structural transition. Table 1 summarizes the structures of all the PVACl−SC_nS complexes formed at different pH values (pH = 5.9−12.0) and different surfactant tail length (*n* = 9−12). A comparison of these structures more clearly indicated that the structural transition from 2D distorted hexagonal to lamellar and then to 2D hexagonal could be induced either by increasing the pH values of complexation or by decreasing the surfactant tail length. However, under extreme conditions such as *n* = 9 with largest mean curvature of surfactant and weakest hydrophobic interactions during complexation, the increase in pH from 5.9 to 12.0 did not induce the structural transition. All the PVACl−SC_9S complexes formed at pH = 5.9−12.0 produced a 2D hexagonal structure.

Figure 5 shows the SAXS profiles of PVACl−$SC_{14}S$ complexes formed at different pH values (3.3−8.9). All three curves showed two scattering peaks with a spacing ratio of 1:2, indicating a lamellar structure had been formed. Furthermore, the increase in pH did not shift the scattering peak positions. This means that when the surfactant tail length was long enough (e.g., $n \geq 14$), the increase in pH values of complexation would also

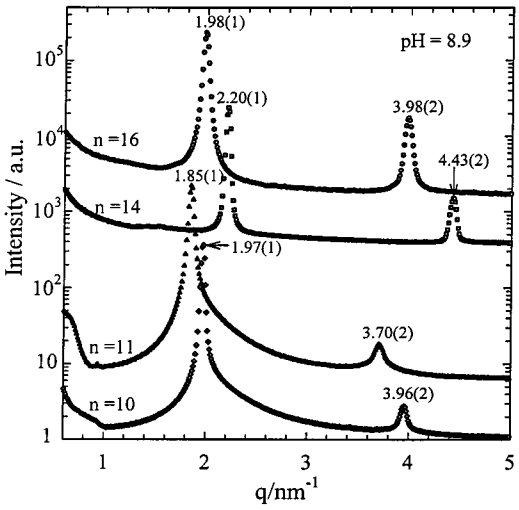

Figure 6. Comparison of the SAXS profiles of PVACl−SC_nS complexes with lamellar structures formed at pH = 8.9, but different n values of 10, 11, 14, and 16.

not induce a structural transition. As shown in Table 1, the lamellar structures have been formed in PVACl−SC_nS complexes with shorter surfactant tail length, e.g., $n = 10-11$. The increase in n to 12 induced a structural transition from lamellar to a 2D distorted hexagonal packing. Why did a further increase in n to 14 produce a lamellar structure again? Figure 6 shows a comparison of SAXS curves of PVACl−SC_nS complexes with lamellar structures formed at pH = 8.9 but different n = 10, 11, 14, and 16. Obviously, the lamellar structure formed by long-tailed surfactants of $SC_{14}S$ and $SC_{16}S$ was actually different from that formed by short-tailed surfactants of $SC_{11}S$ and $SC_{10}S$ in PVACl−SC_nS complexes. If the surfactant molecules had the same arrangement in the lamellar structures formed in complexes, the lamellar spacing would increase with increasing surfactant tail length. For example, the lamellar spacing of 3.40 nm formed at $n = 11$ was larger than the lamellar spacing of 3.19 nm formed at $n = 10$. The difference in lamellar spacing produced by one CH_2 group in surfactant tails was equal to 0.21 nm. Considering the bilayer arrangement of C_nS ions in the lamellar structure, this difference in lamellar spacing implicated a projected C−C link length of 1.05 Å, suggesting that the surfactant chains in the complexes were nearly fully extended and perpendicular to the lamellar surface. However, when the carbon atom number n was increased to 14, the lamellar spacing became even smaller, e.g., 2.86 nm. By further increasing n to 16, the long period of the lamellar increased again to 3.17 nm. In this group, the difference of the lamellar spacing produced by one CH_2 group in surfactant tails was equal to 1.55 Å, implicating an average projected C−C link length of 0.78 Å in the lamellar arrangement. This result indicated that the alkyl chains of surfactant in the complexes were not fully extended and possibly tilted with respect to the lamellar surface. That is why the lamellar spacing in complexes formed by $SC_{14}S$ and $SC_{16}S$ could be even smaller than that formed by $SC_{10}S$ and $SC_{11}S$. The longer the surfactant tails, the stronger are the hydrophobic interactions among the alkyl chains when forming complexes; thus, the bilayer arrangement among the long alkyl chains could be partially overlapped or tilted due to the space hindrance.

Conclusions

The interactions between linear PVACl chains and oppositely charged SC_nS surfactants could produce complexes with highly ordered nanostructures. A novel phase structure of 2D distorted hexagonal packing of deformed cylinders or ribbons with $a = b$ and packing angle θ larger than 120° was, for the first time, observed in polyelectrolyte−surfactant complexes. Both increase in pH values for complexation between PVACl and SC_nS solutions and decrease in carbon atom numbers of alkyl chains of SC_nS could induce a phase structural transition of the formed complexes, from 2D distorted hexagonal to lamellar and then to 2D hexagonal phase. This phase transition could be attributed to the increase in mean curvature at the polar/apolar interface (or ratio of area of polar group to volume of alkyl chains) of C_nS ions in the complexes caused by either decrease in charge density of PVA chains (headgroup swollen of surfactant) or shortening of surfactant tails. Two different lamellar phases could be formed in PVACl−SC_nS complexes by changing the surfactant tail length under certain pH values. The alkyl chains of surfactant were fully extended and perpendicular to the lamellar surface in complexes formed by surfactants with medium alkyl chain length, e.g., $n = 10$ and 11, while the alkyl chains of surfactant were partially overlapped or tilted to the lamellar surface in complexes formed by surfactants with long alkyl chain length, e.g., $n = 14$ and 16.

Acknowledgment. B.C. gratefully acknowledges the support of this work by, Polymer Program, the National Science Foundation (DMR9984102), and the Department of Energy for beamline support of X27C (DEFG0299ER45760) at NSLS, BNL. C.B. gratefully acknowledges partial support of this work by the Alexander Von Humboldt Foundation as a Feodor-Lynen Fellow.

References and Notes

(1) Lehn, J. *Angew. Chem., Int. Ed. Engl.* **1988**, *27*, 90; **1990**, *29*, 1304.
(2) Ober, C. K.; Wegner, G. *Adv. Mater.* **1997**, *9*, 17 and references therein.
(3) Zhou, S. Q.; Chu, B. *Adv. Mater.* **2000**, *12*, 545.
(4) Hayakawa, K.; Kwak, J. C. T. In *Cationic Surfactants*; Rubingh, D. N., Holland, P. M., Eds.; Marcel Dekker: New York, 1991; pp 189−248.
(5) Goddard, E. D.; Ananthapadmanabhan, K. P. *Interactions of Surfactants with Polymers and Proteins*; CRC Press: Boca Raton, FL, 1993.
(6) Konop, A. J.; Colby, R. H. *Langmuir* **1999**, *15*, 58.
(7) Bronich, T. K.; Kabanov, A. V.; Kabanov, V. A.; Yu, K.; Eisenberg, A. *Macromolecules* **1997**, *30*, 3519.
(8) Kabanov, A. V.; Bronich, T. K.; Kabanov, V. A.; Yu, K.; Eisenberg, A. *J. Am. Chem. Soc.* **1998**, *120*, 9941.
(9) Lysenko, E. A.; Bronich, T. K.; Eisenberg, A.; Kabanov, V. A.; Kabanov, A. V. *Macromolecules* **1998**, *31*, 4511.
(10) Okuzaki, H.; Osada, Y. *Macromolecules* **1995**, *28*, 380.
(11) Mironov, A. V.; Starodoubtsev, S. G.; Khokhlov, A. R.; Dembo, A. T.; Yakunin, A. N. *Macromolecules* **1998**, *31*, 7698.
(12) Antonietti, M.; Kaul, A.; Thunemann, A. *Langmuir* **1995**, *11*, 2633.
(13) Antonietti, M.; Maskos, M. *Macromolecules* **1996**, *29*, 4199.
(14) Antonietti, M.; Radloff, D.; Wiesner, U.; Spiess, H. W. *Macromol. Chem. Phys.* **1996**, *197*, 2713.
(15) Sokolov, E. L.; Yeh, F.; Khokhlov, A. R.; Chu, B. *Langmuir* **1996**, *12*, 6229.
(16) Yeh, F.; Solokov, E. L.; Khokhlov, A. R.; Chu, B. *J. Am. Chem. Soc.* **1996**, *118*, 6615.
(17) Zhou, S. Q.; Burger, C.; Yeh, F.; Chu, B. *Macromolecules* **1998**, *31*, 8157.
(18) Zhou, S. Q.;Yeh, F. J.; Burger, C.; Chu, B. *J. Polym. Sci., Polym. Phys. Ed.* **1999**, *37*, 2165.

(19) Zhou, S. Q.; Yeh, F. J.; Burger, C.; Chu, B. *J. Phys. Chem. B* **1999**, *103*, 2107.
(20) Zhou, S. Q.; Hu, H. B.; Burger, C.; Chu, B. *High Performance Polym.* Submitted for publication.
(21) Funari, S. S.; Rapp, G. *Proc. Natl. Acad. Sci. U.S.A.* **1999**, *96*, 7756.
(22) Chu, B.; Harney, P. J.; Li, Y.; Linliu, K.; Yeh, F.; Hsiao, B. S. *Rev. Sci. Instrum.* **1994**, *65*, 597.
(23) Auvray, X.; Petipas, C.; Anthore, R.; Rico, I.; Lattes, A. *J. Phys. Chem.* **1989**, *93*, 7458.
(24) Kekicheff, P. *J. Colloid Interface Sci.* **1989**, *131*, 133.
(25) Seddon, J. M. *Biochim. Biophys. Acta* **1990**, *1031*, 1.
(26) Mariani, P.; Luzzati, V.; Delacroix, H. *J. Mol. Biol.* **1988**, *204*, 165.

MA001277M